

Supporting Information:

Towards Understanding Solvation Effects on the Conformational Entropy of Non-rigid Molecules

Johannes Gorges,[†] Stefan Grimme,[†] Andreas Hansen^{*,†} and Philipp Pracht^{*,‡}

[†]*Mulliken Center for Theoretical Chemistry, Institute for Physical and Theoretical Chemistry, University of Bonn, Beringstr. 4, 53115 Bonn, Germany*

[‡]*Institute for Physical Chemistry, RWTH Aachen University, Melatener Str. 20, 52056 Aachen, Germany*

E-mail: hansen@thch.uni-bonn.de,pracht@pc.rwth-aachen.de

S1 Statistical error measures

Statistical measures for a set of data points x_1, \dots, x_n with references r_1, \dots, r_n are:

- Average:

$$\bar{x} = \frac{1}{n} \sum_i^n x_i$$

- Mean deviation(MD):

$$MD = \frac{1}{n} \sum_i^n (x_i - r_i)$$

- Mean absolute deviation(MAD):

$$MAD = \frac{1}{n} \sum_i^n |x_i - r_i|$$

- Standard Deviation (SD):

$$SD = \sqrt{\frac{\sum_i^n (x_i - \bar{x})^2}{n - 1}}$$

- Root-mean-square deviation (RMSD):

$$RMSD = \sqrt{\frac{\sum_i^n |x_i - r_i|^2}{n}}$$

- Pearson correlation coefficient (r):

$$r = \frac{\sum_{i=1}^n (x_i - \bar{x}_i)(r_i - \bar{r}_i)}{\sqrt{\sum_{i=1}^n (x_i - \bar{x}_i)^2(r_i - \bar{r}_i)^2}}$$

S2 Detailed Computational Details

Since the stochastic nature of the molecular dynamics runs in CREST leads to slightly varying results for different runs started on the same input structure, the average of several calculations was taken. The SD was determined for those values to estimate the statistical error. Five individual runs were performed with GFN1- and GFN2-xTB and ten with GFN-FF. In addition, one calculation in all three phases (gas-phase, water, *n*-hexane) was

performed with the GBSA^{S1,S2} model and GFN2 to investigate if large differences could be observed compared to the ALPB model. Gas-phase entropies for the CD25 test set were already calculated in Ref. S3. Values obtained from three individual calculations with GFN2-xTB were taken from this and averaged with three additional calculations performed for this work. For GFN-FF, some bond constraints in the entropy calculation were changed in the development of CREST. For the sake of consistency, the values were calculated again with the newest version of CREST and therefore can deviate in some cases from the respective values in Ref. S3. Some difficulties arose with GFN1-xTB for Tenofovir in all three phases since artificial intramolecular proton transfer was observed. To have a meaningful comparison for the same structural isomer, the respective bond was constrained in the calculation with GFN1 for this molecule. Ritonavir is with 98 atoms and a huge number of possible conformers the current technical limit for the approach at SQM level. Due to the high computational demand, only the mean value of three instead of five individual calculations was taken for Ritonavir at the GFN1- and GFN2-xTB levels.

Conformer energies determined by the GFN methods were benchmarked against DFT values. Therefore, 20 representative conformers of the ensembles obtained with GFN2-xTB in the gas-phase, *n*-hexane, and water, respectively were selected with a k-means and principle component analysis. The procedure was adapted from Ref. S4 where it was applied to conformational energies of transition metal complexes. Singlepoint energies of the GFN methods with ALPB were compared with the composite meta-GGA method r²SCAN-3c^{S5} and the COSMO-RS^{S6,S7} solvation model. This procedure yields also highly accurate solvation energies.^{S8} Calculations were performed using COSMOtherm16^{S9} and TURBOMOLE 7.5^{S10,S11} with the numerical quadrature grid m4^{S12}. In all DFT calculations, the resolution-of-identity (RI)^{S13} approximation using matching default auxiliary basis sets^{S14} was applied to the Coulomb integrals. The Pearson correlation coefficient was used to determine the similarity of the conformational energy ranking between the GFN methods (+ ALPB) and r²SCAN-3c (+ COSMO-RS) reference energies.

S3 Benchmarking Conformational Energies

For some molecules, less than 20 conformers were found within the default energy window of 6 kcal mol⁻¹ at the GFN2-xTB level by CREST and were used for the benchmark study. The respective molecules and the number of conformers are given in Table S1.

Table S1: Number of conformers used for benchmarking conformational entropies of molecules with less than 20 conformers found within a 6 kcal mol⁻¹ window at the GFN2-xTB level . For all other molecules, at least 20 conformers were found and used for the benchmark study.

Molecule	gas-phase	<i>n</i> -hexane	water
Celecoxib	8	12	11
Ibuprofen	14	14	19
Lenalidomid	13	9	11
Au-phosphine	8	14	20
Oxycodone	10	9	12

The obtained Pearson correlation coefficients between GFN methods and r²SCAN-3c are depicted in Figures S1, S2, and S3 for gas, *n*-hexane and water, respectively. In the gas-phase, GFN2 and GFN1 perform moderately well with an average correlation coefficient of 0.57 and 0.60. Anti-correlation with GFN2 is only observed for Sofosbuvir. More outliers are obtained with GFN1, namely Apixaban and Chloroquine. As expected the deviation to the DFT values is larger for the force field with an average correlation of 0.52. Negative correlations are observed for Duloxetine, Oxycodone, and Aripiprazole. Deviations for the transition metal complexes are reasonably small, validating good conformational energies for these systems too.^{S4} Deviations in *n*-hexane are larger on average. This is because the error between the solvation models ALPB and COSMO-RS is added to the error between the methods for the electronic energy. However, the tight-binding methods show slightly better similarity to the DFT values with an average correlation of 0.53 than GFN-FF with 0.49. More anti-correlation than in the gas-phase is also observed. All methods show a negative correlation for Ritonavir and Imatinib.

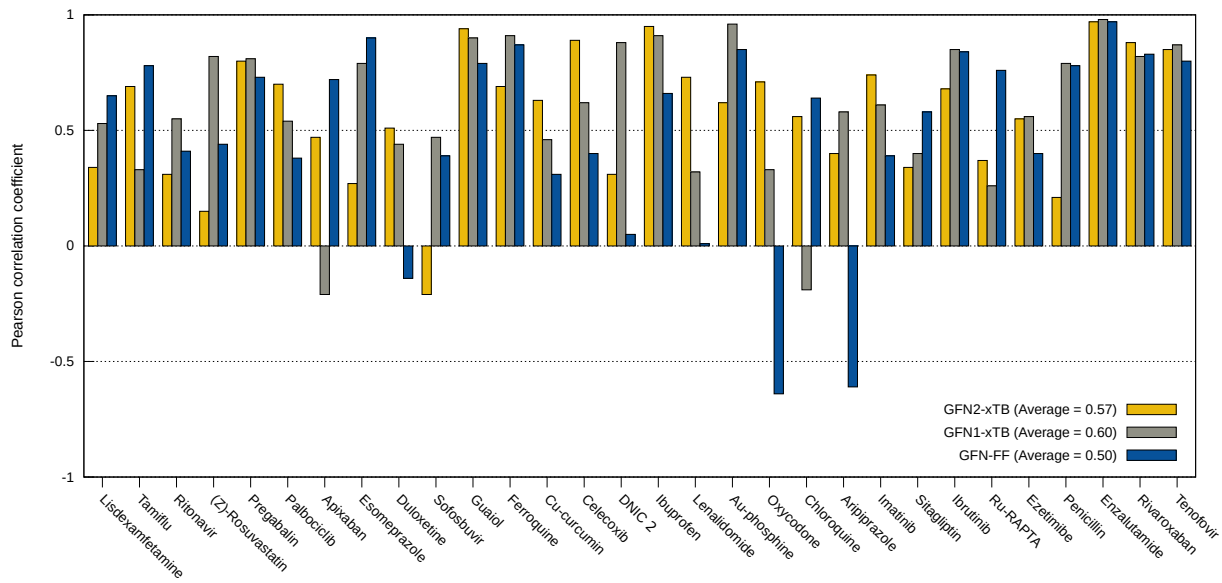


Figure S1: Pearson correlation coefficient for 20 selected conformers between GFN2-, GFN1-xTB, and GFN-FF energies and r^2 SCAN-3c energies for the CD30 set in the gas-phase.

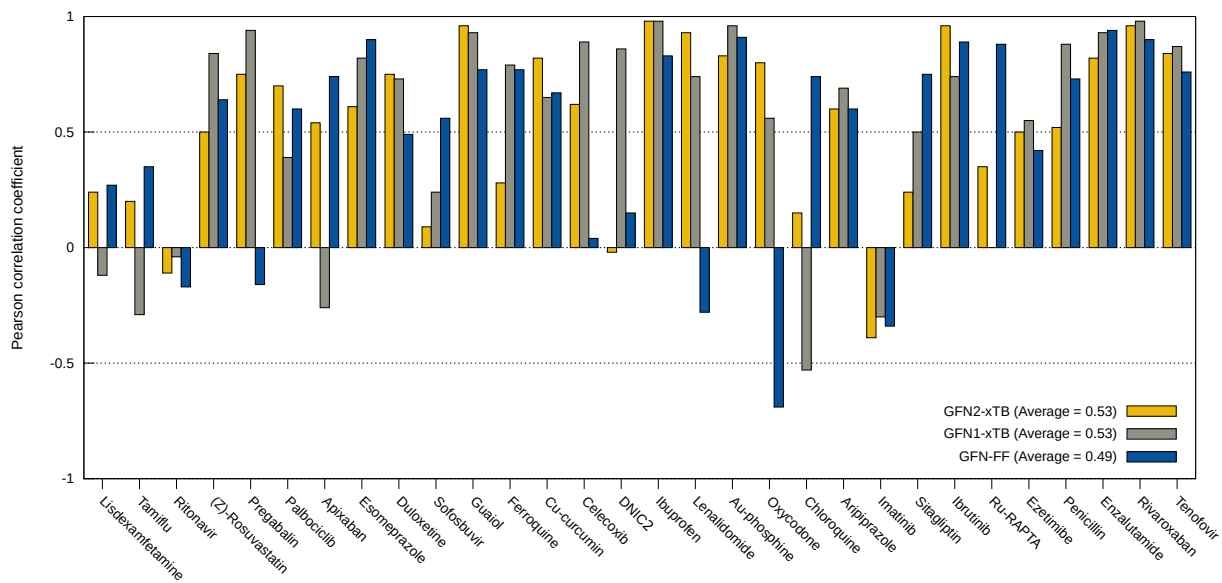


Figure S2: Pearson correlation coefficient for 20 selected conformers between GFN2-, GFN1-xTB, and GFN-FF + ALPB energies and r^2 SCAN-3c + COSMO-RS energies for the CD30 set in implicit *n*-hexane.

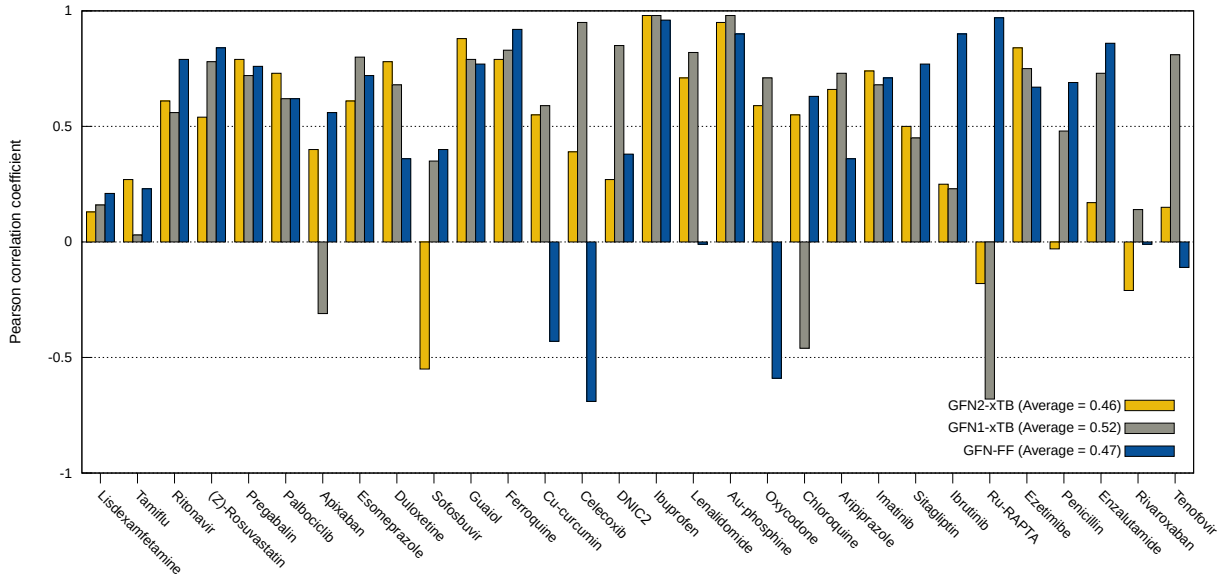


Figure S3: Pearson correlation coefficient for 20 selected conformers between GFN2-, GFN1-xTB, and GFN-FF + ALPB energies and r^2 SCAN-3c + COSMO-RS energies for the CD30 set in implicit water.

In water, the deviations are slightly larger than in the gas-phase and *n*-hexane. Notably, GFN2-xTB shows the on average smallest correlation with $r = 0.46$. GFN1-xTB and GFN-FF perform slightly worse compared to the results in *n*-hexane.

Differences between the ALPB and GBSA implicit solvation model are in general small for GFN2- xTB, as can be seen in Figure S4. With a correlation of $r = 0.55$ (*n*-hexane) and $r = 0.51$ (water), the GBSA model performs for both solvents slightly better than ALPB. Likewise, the $\overline{\text{MAD}}$ of both models is approximately equal in *n*-hexane, whereas in water the $\overline{\text{MAD}}$ of the GBSA model is by 0.1 kcal mol⁻¹ smaller than for ALPB. As the differences are only small, the more theoretically advanced ALPB model was chosen for the calculation of the entropy values.

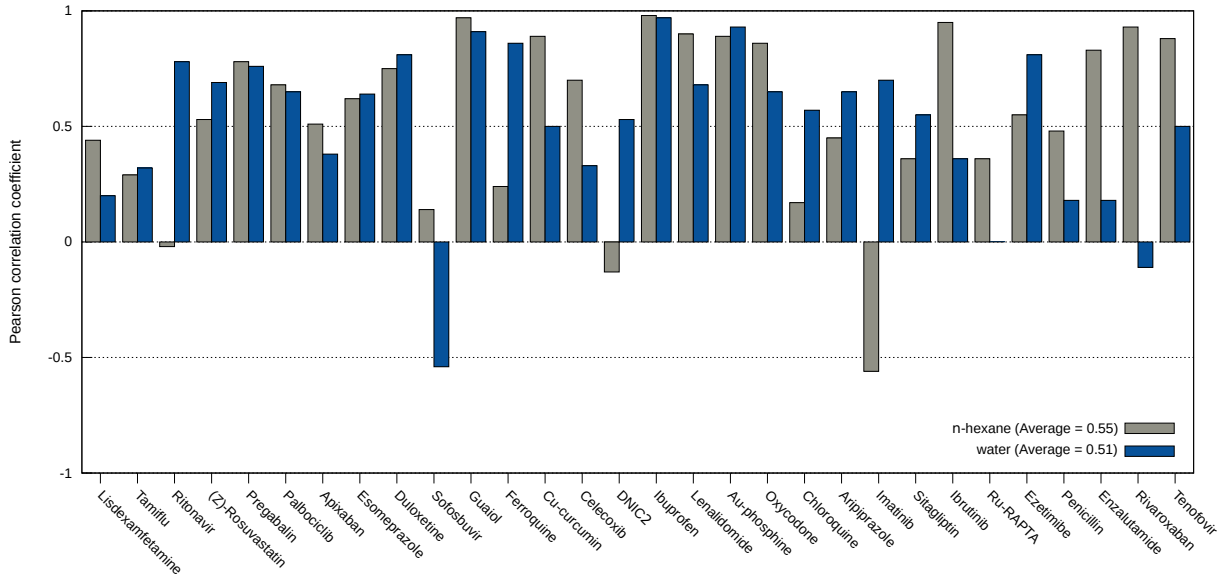


Figure S4: Pearson correlation coefficient for 20 selected conformers between GFN2-xTB energies with GBSA solvation model and r^2 SCAN-3c + COSMO-RS energies for the CD30 set in water and *n*-hexane.

S4 Conformational Entropies at GFN1-xTB and GFN-FF Levels

Conformational entropies at the GFN1-xTB level in the gas-phase, *n*-hexane and aqueous solution for the whole test set are depicted in Figure S5. SDs are comparable to those at the GFN2-xTB level. Some notable differences compared to the GFN2-xTB results are visible. A large entropy gain of $6.3\text{cal mol}^{-1}\text{K}^{-1}$ is predicted for (Z)-Rosuvastatin. For the Cu-curcumin complex, a higher conformational entropy is predicted in water with GFN1-xTB, whereas GFN2 predicts larger entropies in *n*-hexane. Both methods qualitatively agree for molecules of group B and C, except for Ezetimibe. While both SQM methods predict an increase of entropy upon solvation, GFN1 predicts a higher conformational contribution in *n*-hexane, indicating an underestimated effect of the intramolecular H-bond.

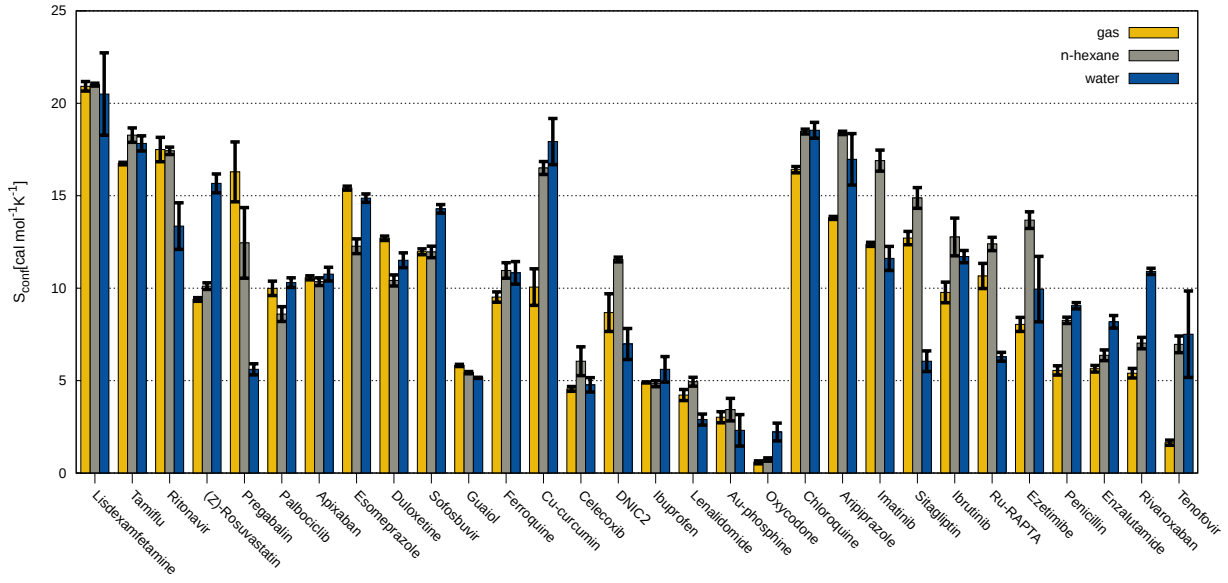


Figure S5: Computed conformational entropy values with GFN1-xTB for the CD30 test set.

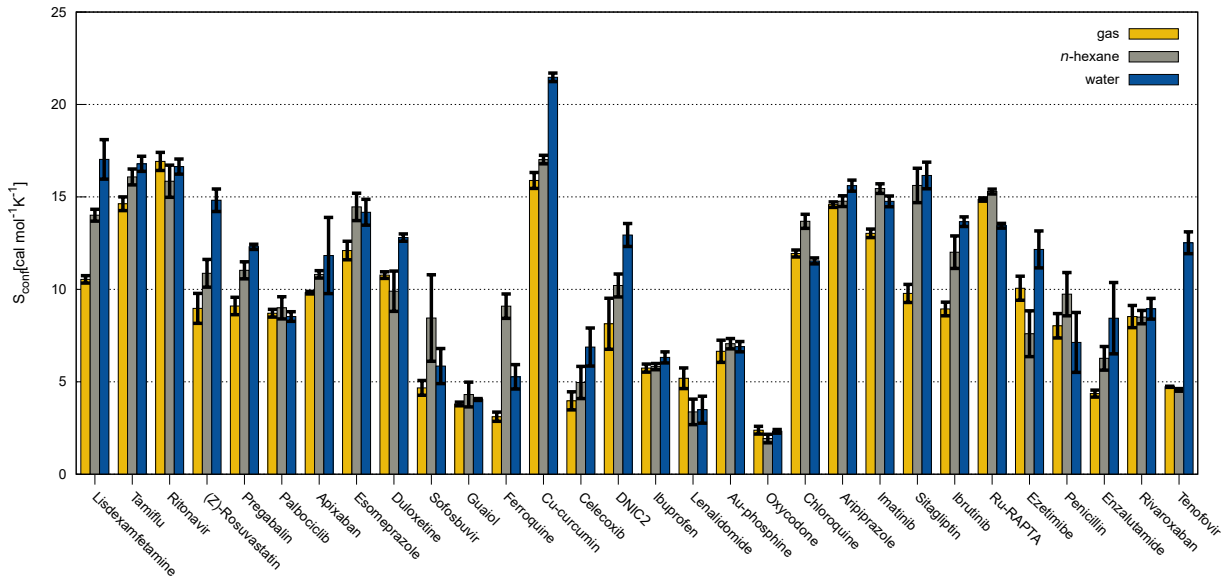


Figure S6: Computed conformational entropy values with GFN-FF for the CD30 test set.

Figure S6 shows the entropies calculated with GFN-FF. SDs are slightly larger compared to the SQM methods, showing errors of around $0.6\text{cal mol}^{-1}\text{K}^{-1}$ for both *n*-hexane and water. The larger fluctuations in *n*-hexane are probably due to the smaller numerical grid employed in the ALPB solvation model for GFN-FF. Further deviations can be observed. Significantly

less entropy is predicted for Lisdexamfetamine in the gas-phase compared to the respective GFN2 and GFN1 calculations. As with GFN1, (Z)-Rosuvastatin is more flexible in water. Cu-curcumin shows much larger entropies than at the SQM levels throughout. Similar to GFN2, an entropy gain in water is observed for DNIC 2, Sofosbuvir, and Esomeprazole. For molecules of groups B and C, qualitative trends are well reproduced. Notably, for Aripiprazole a small entropy gain is observed in water but not in *n*-hexane. This is probably due to the intramolecular H-bond in the ensemble (see Table S3), which is not predicted by the other methods. Opposed to the other methods, Ibrutinib is most flexible in water and penicillin in *n*-hexane. In conclusion, the force field gives in many cases qualitatively different results compared to the SQM methods.

S5 Average Solvent Accessible Surface Area of Conformer Ensembles

Solvent accessible surface areas (SASAs) for the clustered SEs at the GFN2-xTB level were determined with a GFN2-xTB(ALPB) singlepoint calculation in *n*-hexane and water. They were Boltzmann weighted according to Eq. (3) at the respective theory level at which their geometry was optimized and summed to obtain an averaged SASA (SASA_{Bw}) for each molecule in each phase.

On average, SASA_{Bw} increases from gas phase to *n*-hexane by 13.7 \AA^2 and decreases by 0.5 \AA^2 from gas-phase to water. For molecules that exhibit intramolecular stacking, the implicit solvent model ALPB predicts this trend here correctly.

Table S2: SASAs with respect to water and *n*-hexane for clustered SEs at the GFN2-xTB level of the CD30 set in all three phases. They are Boltzmann weighted at the GFN2-xTB (+ ALPB) level of theory at which their geometries were optimized.

	SASA _{Bw} / (<i>n</i> -hexane) Å ²		SASA _{Bw} (water) / Å ²	
	gas	<i>n</i> -hexane	gas	water
Lisdexamfetamine	364.72	387.63	411.63	427.04
Tamiflu	431.68	444.52	497.38	497.99
Ritonavir	731.3	783.52	741.85	723.13
(Z)-Rosuvastatin	489.16	499.7	558.81	557.36
Pregabalin	260.48	260.96	312.84	311.7
Palbociclib	534.75	540.95	606.08	603.81
Apixaban	554.6	556.71	643.91	646.47
Esomeprazole	385.71	407.42	480.25	441.63
Duloxetine	385.41	396.92	464.82	451.58
Sofosbuvir	523.3	540.06	581.14	600.73
Guaiol	340.69	341.41	394.81	395.06
Ferroquine	440.96	440.93	500.22	497.78
Cu-curcumin	452.25	505.76	515.47	523.53
Celecoxib	427.07	427.7	501.98	502.09
DNIC 2	279.9	282.07	335.37	334.81
Ibuprofen	320.57	321.35	380.91	380.8
Lenalidomide	320.37	321.24	381.8	378.03
Au-phosphine	415.59	420.8	484.26	487.87
Oxycodone	359.92	360.83	418.06	416.46
Chloroquine	408.99	423.02	465.28	472.58
Aripiprazole	462.73	499.21	529.31	527.31
Imatinib	525.47	555.86	578.16	578.3
Sitagliptin	383.12	398.66	441.95	438.81
Ibrutinib	502.35	516.49	574.17	584.05
Ru-RAPTA	491.3	500.42	541.98	549.14
Ezetimibe	448.27	473.91	511.85	517.67
Penicillin	379.58	400.14	441.66	433.35
Enzalutamide	494.97	496.8	575.02	576.18
Rivaroxaban	423.58	443.93	482.39	482.31
Tenofovir	322.05	322.67	380.16	382.36
average	428.7	442.39	491.12	490.66

S6 Average Number of Hydrogen Bonds

To investigate the effect of intramolecular hydrogen bonding on the conformational entropy, H-bond analyses were performed for all obtained conformer ensembles of the CD30 set. Since the discussion of conformational entropies is mainly based on molecular geometries, H-bonds were determined according to geometrical criteria. As they occur intramolecular, relatively loose criteria were chosen. For the donor-acceptor distance, a cut-off of 3.5 Å was chosen and for the H-bond angle, a cut-off of 40 °. These criteria are based on the ones chosen in Ref. S15 but were converted because hydrogen bond angles are differently defined in VMD compared to the definition given there. In addition, only polar atoms (N, O, F, and S) were considered. Analyses were performed with VMD 1.9.^{S16} For each conformer of the investigated ensembles, the number of H-bonds was determined. To allow a meaningful comparison between the number of H-bonds of the ensembles, which consist of different numbers of conformers, they were summed up for each ensemble according to a Boltzmann distribution. Therefore, they were multiplied by the thermal population p_i of the respective conformer according to Eq. (3) and then added. The determined Boltzmann weighted H-bond sum $N(\text{H-bond})_{\text{Bw}}$ is meant to give insight into how much conformers exhibiting H-bonds are populated within the ensemble and thus affect the conformational entropy.

19 molecules of the CD30 set exhibit intramolecular H-bonds in at least one obtained SE. The determined Boltzmann-weighted H-bond sums $N(\text{H-bond})_{\text{Bw}}$ of these molecules are tabulated in Table S3. All three methods predict significantly fewer H-bonds in the medium with a larger dielectric constant. This shows, that the employed implicit solvation model ALPB predicts this expected trend correctly. While the tight-binding methods give similar results, the force field predicts much larger values. This is most prominent for Tamiflu, Aripiprazole, Sitagliptin, Duloxetine, Penicillin, and Cu-curcumin, for which only GFN-FF shows significantly populated conformers including H-bonds. This is probably due to the special H-bond term in its energy expression^{S17} which seems to overestimate the energy gain from hydrogen bonding.

Table S3: Boltzmann-weighted H-bond sum $N(\text{H-bond})_{\text{Bw}}$ for the determined SEs of molecules of the CD30 set, for which at least one method predicted intramolecular H-bonding (threshold of 0.1).

molecule	GFN2				GFN1			GFN-FF			
	gas	<i>n</i> -hexane		water	gas	<i>n</i> -hexane	water	gas	<i>n</i> -hexane	water	
		ALPB	GBSA								
Lisdexamfetamine	0.44	0.21	0.14	0.28	0.24	0.48	0.21	0.01	1.31	1.46	1.05
Tamiflu	0.00	0.00	0.00	0.00	0.00	0.00	0.00	0.00	0.71	0.63	0.77
Ritonavir	2.01	2.03	2.09	1.98	1.89	2.17	2.09	0.62	3.23	3.31	3.25
(Z)-Rosuvastatin	1.96	1.35	1.20	1.10	1.08	1.17	1.05	0.31	2.86	2.86	2.49
Pregabalin	0.05	0.08	0.10	0.10	0.20	0.13	0.67	0.96	0.96	0.93	0.86
Esomeprazole	0.00	0.03	0.05	0.01	0.04	0.00	0.00	0.01	0.03	0.09	0.14
Duloxetine	0.00	0.00	0.00	0.03	0.00	0.05	0.03	0.01	0.40	0.42	0.45
Sofosbuvir	0.03	0.03	0.06	0.00	0.01	0.10	0.06	0.31	1.99	1.96	1.94
Ferroquine	0.98	0.97	0.97	0.98	0.96	0.96	0.97	0.97	1.00	1.00	1.00
Cu-curcumin	0.00	0.00	0.00	0.00	0.00	0.00	0.00	0.00	0.21	0.00	0.00
DNIC 2	0.22	0.09	0.11	0.03	0.02	0.85	0.70	0.00	1.98	1.30	1.63
Oxycodone	0.00	0.00	0.00	0.00	0.00	0.01	0.00	0.00	1.00	0.99	0.95
Chloroquine	0.19	0.04	0.05	0.13	0.14	0.02	0.00	0.00	0.87	0.82	0.90
Aripiprazole	0.00	0.00	0.00	0.00	0.00	0.00	0.00	0.00	0.60	0.62	0.11
Imatinib	0.26	0.13	0.26	0.15	0.34	0.25	0.03	0.00	0.56	0.44	0.59
Sitagliptin	0.00	0.00	0.00	0.00	0.00	0.02	0.00	0.00	0.66	0.68	0.02
Ezetimibe	0.29	0.61	0.60	0.08	0.09	0.80	0.42	0.03	0.98	0.99	0.84
Penicillin	0.00	0.00	0.00	0.00	0.00	0.00	0.00	0.00	0.04	0.18	0.01
Tenofovir	1.00	1.00	1.00	0.22	0.80	1.00	1.00	0.97	0.99	1.00	0.67
average	0.39	0.35	0.35	0.27	0.31	0.42	0.38	0.22	1.07	1.04	0.93

S7 Correlation with the Empirical Flexibility Measure

Some simulation settings in the CREST entropy mode can be derived from the flexibility of the respective molecule. For this purpose, an empirical molecular flexibility measure ξ_f was introduced in Ref. S3.

The correlation plots between $S_{\text{conf}} / N_{\text{at}}$ (the number of atoms of the respective molecule) and the empirical flexibility measure for the GFN methods is shown in Figure S7. In general, only mediocre correlation is obtained at the GFN2 level, showing values from 0.59 (*n*-hexane) to 0.71 (water). The largest deviations from a perfect correlation are observed for Ferroquine, DNIC 2, the Au-phosphine complex, and Oxycodone. Since ξ_f was developed with organic molecules in mind, there appears to be greater deviation for transition metal complexes. GFN1-xTB has a rather high correlation of $r = 0.83$ and $r = 0.71$ for the gas-phase and *n*-hexane, respectively, whereas in water it is significantly lower. Notably, the transition

metal compounds show a much better correlation than with GFN2. Outliers are here Au-phosphine, Tenofovir, and Oxycodone.

GFN-FF has correlations of similar magnitude as GFN2 for the gas-phase and water, whereas in *n*-hexane it is higher. The largest deviations from linear behavior are observed for Sofosbuvir, Ferroquine and Oxycodone.

The correlation plots show that S_{conf} depends entirely on the PES and the empirical flexibility measure based on the geometry is only a rough estimation tool for it. Note that changes in the PES upon solvation are not reflected accurately in ξ_f as it is only based on the structural descriptors for the minimum structure of the molecule.

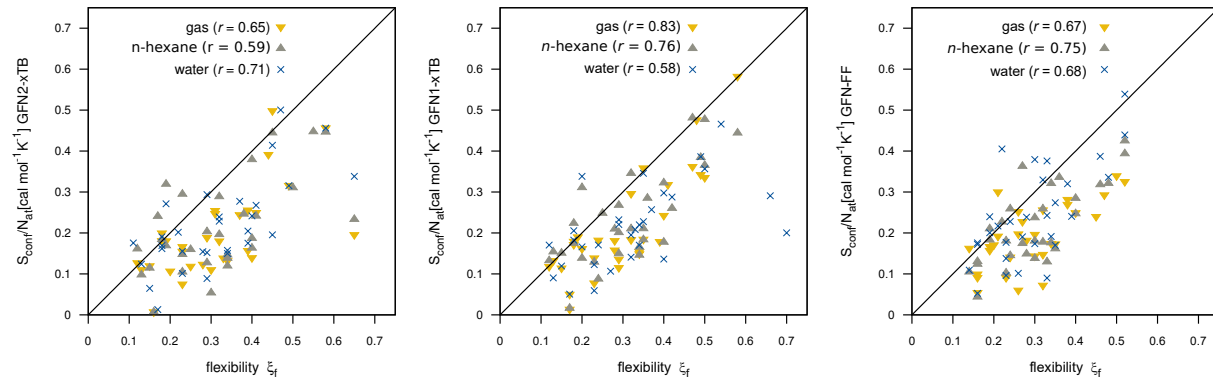


Figure S7: Correlation plots between $S_{\text{conf}}/N_{\text{at}}$ and the empirical flexibility measure ξ_f at GFN1-, GFN2-xTB, and GFN-FF levels in gas, *n*-hexane, and water. The respective Pearson correlation coefficients r are provided in parentheses.

S8 Comparison with explicit solvation

Geometries obtained with the ALPB implicit solvation model were compared to geometries determined with explicit solvation for two molecules, namely Aripiprazole and Tenofovir. Therefore, explicit solvated molecular clusters with ten water or *n*-hexane solvent molecules were generated with the QCG algorithm^{S18}. The lowest conformer of the clusters was determined with CREST at the GFN2-xTB level of theory.

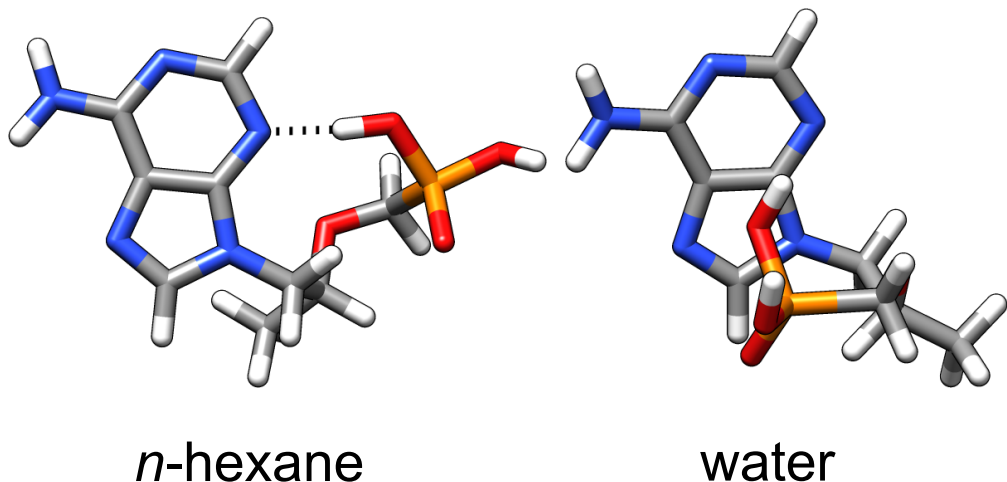


Figure S8: Optimized geometries of lowest found conformer for Tenofovir with explicit solvation of 10 solvent molecules for *n*-hexane and water obtained with the QCG algorithm at the GFN2-xTB level of theory. Solvent molecules are omitted for clearer visibility. Although the root-mean-square deviations (RMSDs) of the heavy atom positions to the geometries obtained with implicit solvation (Figure 5) are with 0.22 Å (*n*-hexane) and 0.91 Å (water) rather large, qualitative agreement with respect to the intramolecular H-bond is observed.

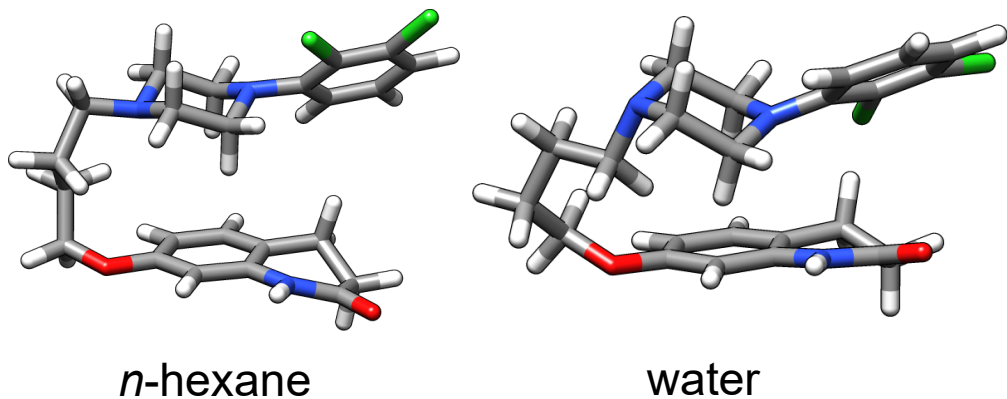


Figure S9: Optimized geometries of lowest found conformer for Aripiprazole with explicit solvation of 10 solvent molecules for *n*-hexane and water obtained with the QCG algorithm at the GFN2-xTB level of theory. Solvent molecules are omitted for clearer visibility. Although the RMSDs to the geometries obtained with implicit solvation (Figure 5) are with 1.30 Å (*n*-hexane) and 1.29 Å (water) rather large, qualitative agreement with respect to the intramolecular stacking is observed.

S9 Solvation Free Energies

Solvation free energies for the CD30 set were computed as difference between the Boltzmann weighted ensemble energy of the 20 conformers at the r²SCAN-3c (+ COSMO-RS) level in gas-phase, *n*-hexane, and water, respectively. The difference in conformational entropy between the phases computed at the GFN2-xTB level was added according to the Gibbs free energy equation $\Delta G_{\text{conf}} = -T \cdot \Delta S_{\text{conf}}$. Note, that solvation free energies computed by COSMO-RS, already contain an entropy dependence due to their fit to experimental free energies. Therefore, it is currently not clear if adding ΔS_{conf} would amount to some double counting.

Table S4: Computed solvation free energies ΔG_{solv} in kcal mol⁻¹ for the conformer ensembles of the CD30 set at the r²SCAN-3c (+ COSMO-RS) level with and without inclusion of the conformational entropy contribution $\Delta G_{\text{conf}} = -T \cdot \Delta S_{\text{conf}}$ at the GFN2-xTB level to the free energy at 298.15 K.

	<i>n</i> -hexane		water	
	ΔG_{solv}	$\Delta G_{\text{solv}} + \Delta G_{\text{conf}}$	ΔG_{solv}	$\Delta G_{\text{solv}} + \Delta G_{\text{conf}}$
Lisdexamfetamine	-10.56	-9.90	-11.95	-11.98
Tamiflu	-13.41	-13.34	-15.62	-15.62
Ritonavir	-25.88	-26.79	-15.14	-16.54
(Z)-Rosuvastatin	-18.07	-15.76	-12.91	-11.15
Pregabalin	-9.99	-9.92	-7.58	-7.58
Palbociclib	-21.95	-21.75	-20.16	-19.96
Apixaban	-24.59	-24.66	-27.11	-27.28
Esomeprazole	-16.99	-17.02	-13.94	-14.37
Duloxetine	-13.53	-13.44	-5.40	-5.61
Sofosbuvir	-16.52	-16.99	-20.18	-20.88
Guaiol	-8.71	-8.62	-3.07	-3.08
Ferroquine	-17.94	-17.08	-11.99	-11.66
Cu-curcumin	-24.90	-28.26	-29.27	-31.87
Celecoxib	-16.32	-16.27	-13.48	-12.83
DNIC 2	-7.74	-8.01	-5.45	-6.48
Ibuprofen	-8.12	-8.19	-5.29	-5.55
Lenalidomide	-14.12	-14.00	-20.33	-20.46
Au-phosphine	-20.21	-20.57	-15.61	-15.92
Oxycodone	-13.63	-13.64	-11.57	-11.65
Chloroquine	-13.08	-13.85	-6.78	-7.11
Aripiprazole	-18.27	-20.37	-14.04	-13.81
Imatinib	-23.80	-26.42	-21.29	-22.02
Sitagliptin	-13.52	-13.97	-15.34	-15.02
Ibrutinib	-20.82	-21.53	-18.21	-17.57
Ru-RAPTA	-22.86	-23.60	-25.38	-25.98
Ezetimibe	-17.95	-18.20	-16.17	-17.07
Penicillin	-14.97	-15.15	-18.20	-19.49
Enzalutamide	-19.54	-20.04	-16.35	-17.05
Rivaroxaban	-19.51	-19.58	-22.52	-22.96
Tenofovir	-13.25	-13.33	-20.71	-21.27
average	-16.69	-17.01	-15.37	-15.66

S10 Detailed Results

Table S5: Mean deviation (MD) and mean absolute deviation (MAD) in kcal mol^{-1} for 20 relative conformer energies of each molecule of the CD30 set at GFN2-xTB level in comparison to $r^2\text{SCAN-3c}$ (+ COSMO-RS) single-point energies.

molecule	gas		<i>n</i> -hexane				water			
			ALPB		GBSA		ALPB		GBSA	
	MD	MAD	MD	MAD	MD	MAD	MD	MAD	MD	MAD
Lisdexamfetamine	-1.53	1.65	-1.82	1.84	-1.89	1.92	-1.85	1.93	-1.86	1.98
Tamiflu	-0.47	0.75	-0.63	1.07	-1.02	1.33	-2.52	2.67	-2.61	2.74
Ritonavir	-3.63	3.93	-1.84	2.57	-2.26	2.68	-3.70	3.88	-3.02	3.19
(Z)-Rosuvastatin	-1.74	2.03	-2.33	2.61	-1.91	2.20	-2.64	2.84	-2.47	2.63
Pregabalin	-1.06	1.16	-4.13	4.22	-3.95	4.00	-0.53	1.03	-0.63	1.06
Palbociclib	-0.30	1.13	-0.33	1.24	-0.67	1.03	-0.89	1.09	-0.68	1.02
Apixaban	-0.67	0.82	-0.86	1.03	-0.83	1.10	-1.18	1.29	-1.21	1.30
Esomeprazole	0.24	1.53	-0.63	1.90	-1.02	1.97	0.92	1.11	1.19	1.30
Duloxetine	-1.83	1.97	-1.92	2.02	-2.41	2.43	-0.62	0.92	-0.46	0.83
Sofosbuvir	-5.43	5.79	-3.22	3.91	-4.05	4.77	-5.76	6.22	-5.68	6.16
Guaiol	0.23	0.45	0.34	0.50	0.33	0.45	0.16	0.54	0.13	0.53
Ferroquine	-4.17	4.17	-4.06	4.76	-2.85	3.92	-3.67	3.67	-3.76	3.77
Cu-curcumin	0.53	1.36	-0.03	0.64	-0.32	0.65	0.61	1.17	0.35	1.02
Celecoxib	0.22	0.24	0.32	0.56	0.17	0.55	-0.75	0.87	-0.63	0.92
DNIC 2	-2.61	3.46	-1.99	3.63	-2.95	4.21	-3.64	3.97	-2.75	3.29
Ibuprofen	-0.38	0.38	-0.44	0.44	-0.42	0.43	-0.16	0.29	-0.16	0.30
Lenalidomide	-1.16	1.16	-0.37	0.53	-0.63	0.69	0.31	1.28	0.43	1.40
Au-phosphine	-0.93	1.40	-0.49	1.00	-0.54	0.94	-0.23	0.57	-0.23	0.64
Oxycodone	-2.43	3.14	-2.74	3.60	-2.80	3.46	-2.87	3.68	-2.88	3.58
Chloroquine	-1.42	1.71	-1.79	1.96	-1.53	1.68	-1.22	1.48	-1.15	1.45
Aripiprazole	-3.07	3.26	-3.12	3.16	-1.74	1.82	-4.00	4.23	-4.00	4.23
Imatinib	-0.88	1.22	-1.07	1.58	-1.82	2.22	0.08	0.94	-0.17	1.05
Sitagliptin	-2.72	2.85	-2.01	2.07	-2.63	2.69	-1.48	1.90	-1.51	1.86
Ibrutinib	-0.87	0.97	-1.02	1.02	-0.90	1.00	-1.18	1.90	-1.30	1.77
Ru-RAPTA	-1.92	2.41	-3.04	3.13	-2.28	2.37	-6.92	7.04	-7.33	7.38
Ezetimibe	-1.32	1.48	-1.39	1.71	-1.44	1.74	-1.37	1.39	-1.24	1.31
Penicillin	-1.69	2.11	-1.75	1.86	-2.86	2.90	-1.76	2.29	-2.33	2.42
Enzalutamide	-0.18	0.43	0.08	0.68	0.09	0.36	-0.32	0.72	-0.31	0.71
Rivaroxaban	-0.90	1.37	0.17	0.46	-0.12	0.66	-1.98	2.78	-2.39	2.90
Tenofovir	-2.41	2.47	-1.74	2.03	-1.81	1.97	-3.74	4.18	-3.44	3.60
average	-1.5	1.9	-1.5	1.9	-1.5	1.9	-1.8	2.3	-1.7	2.2

Table S6: Mean deviation (MD) and mean absolute deviation (MAD) in kcal mol^{-1} for relative conformer energies of each molecule of the CD30 set at GFN1-xTB and GFN-FF level (+ ALPB) in comparison to $r^2\text{SCAN-3c}$ (+ COSMO-RS) single-point energies. For the averaged MDs and MADs, DNIC 2 has been removed from the GFN-FF results.

molecule	gas				<i>n</i> -hexane				water			
	GFN1		GFN-FF		GFN1		GFN-FF		GFN1		GFN-FF	
	MD	MAD	MD	MAD	MD	MAD	MD	MAD	MD	MAD	MD	MAD
Lisdexamfetamine	-1.79	1.84	-0.31	1.11	-1.16	1.42	0.16	1.55	-0.35	1.27	0.52	1.36
Tamiflu	-1.11	1.36	0.56	0.95	-1.07	1.46	-0.48	1.13	-2.05	2.23	-2.15	2.42
Ritonavir	-2.51	2.95	1.67	3.04	-2.06	2.91	1.77	3.67	-3.12	3.55	4.87	5.06
(Z)-Rosuvastatin	-1.17	1.49	-0.92	1.56	-1.19	1.68	0.39	2.19	-1.34	1.80	-0.91	1.46
Pregabalin	-1.35	1.35	0.48	1.18	-3.20	3.20	-4.10	4.74	-0.33	1.09	0.03	0.84
Palbociclib	-0.30	1.21	-0.43	1.41	-0.59	1.52	-0.50	1.41	-1.10	1.25	-0.19	1.21
Apixaban	-0.58	1.03	0.01	0.78	-0.88	1.40	0.37	0.84	-0.94	1.49	-0.14	0.87
Esomeprazole	-0.94	1.39	0.25	0.66	-0.78	1.35	-0.34	0.97	0.83	0.90	1.23	1.31
Duloxetine	-2.02	2.16	-1.29	2.40	-2.18	2.23	-1.63	2.02	-0.79	1.09	-0.04	1.33
Sofosbuvir	-2.82	3.20	-0.24	3.72	-1.89	2.93	4.08	5.33	-5.49	5.63	0.25	3.95
Guaiol	-0.08	0.51	1.25	1.35	-0.03	0.50	1.46	1.76	-0.33	0.86	0.94	1.33
Ferroquine	-4.47	4.47	-1.53	2.51	-5.01	5.05	-3.95	4.20	-3.33	3.60	-0.89	1.42
Cu-curcumin	0.35	1.45	0.44	1.82	-0.01	1.00	0.21	0.98	-0.36	1.02	-0.44	1.65
Celecoxib	0.10	0.38	1.24	1.42	-0.25	0.38	1.83	2.25	-0.05	0.23	1.05	2.79
DNIC 2	-2.59	2.82	119.97	120.47	-2.24	2.50	116.96	117.33	-2.57	2.60	78.87	80.27
Ibuprofen	-0.65	0.65	-0.89	0.97	-0.66	0.66	-0.69	0.82	-0.11	0.32	-0.33	0.47
Lenalidomide	-1.72	1.72	0.78	2.78	-0.82	0.96	1.72	3.89	-0.83	0.86	0.85	2.69
Au-phosphine	1.05	1.10	-0.57	1.09	1.11	1.17	-0.14	0.95	2.08	2.12	-0.47	0.89
Oxycodone	-2.46	3.80	-1.27	5.81	-3.22	4.26	-2.53	6.02	-4.05	4.45	-3.02	4.94
Chloroquine	-1.78	2.18	-0.70	1.42	-1.52	2.26	-0.25	0.93	-1.07	1.98	0.31	1.13
Aripiprazole	-3.27	3.29	-1.75	3.23	-2.42	2.42	-2.16	2.17	-3.19	3.19	-2.76	3.13
Imatinib	-0.63	1.46	-0.42	1.82	-0.72	1.54	0.10	1.56	0.38	0.93	0.25	0.82
Sitagliptin	-2.38	2.53	-1.42	1.92	-1.82	1.83	-0.95	1.21	-0.23	1.61	-1.05	1.53
Ibrutinib	-0.63	0.68	0.47	1.01	-0.85	1.04	0.30	0.88	-0.82	1.84	-0.94	1.29
Ru-RAPTA	-3.11	3.13	-1.99	2.31	-3.77	3.77	-2.80	2.85	-6.27	7.34	-1.80	1.94
Ezetimibe	-0.55	1.06	0.76	1.74	-1.38	1.70	0.46	1.45	-0.24	0.86	-0.93	1.23
Penicillin	-0.37	1.43	0.73	1.78	-0.65	1.15	0.54	2.10	-1.02	1.91	1.67	2.43
Enzalutamide	0.64	0.87	1.49	1.62	0.53	0.93	1.63	1.78	0.61	0.71	2.39	2.45
Rivaroxaban	0.65	1.51	0.61	1.73	0.95	1.05	1.05	1.27	-2.39	2.61	0.45	2.89
Tenofovir	-1.13	1.50	-1.68	1.83	0.14	1.32	-2.08	2.37	-0.48	1.52	-1.12	3.54
average	-1.3	1.8	-0.2	1.9	-1.3	1.9	-0.2	2.2	-1.3	2.0	-0.1	2.0

Table S7: Pearson correlation coefficients between r²SCAN-3c (+COSMO-RS) energies and GFN1-, and GFN2-xTB and GFN-FF (+ ALPB) energies for 20 conformers selected from the GFN2-xTB (+ ALPB) conformer ensembles.

molecule	gas			n-hexane						water			
	GFN2	GFN1	GFN-FF	GFN2		GFN1		GFN-FF	GFN2		GFN1		
				ALPB	GBSA	ALPB	ALPB	ALPB	ALPB	ALPB	ALPB	ALPB	ALPB
Lisdexamfetamin	0.33	0.53	0.65	0.24	0.44	-0.12	0.27	0.12	0.20	0.16	0.21		
Tamiflu	0.69	0.33	0.78	0.20	0.29	-0.29	0.35	0.27	0.32	0.03	0.23		
Ritonavir	0.31	0.55	0.41	-0.11	-0.01	-0.04	-0.17	0.61	0.78	0.56	0.79		
(Z)-Rosuvastatin	0.15	0.82	0.44	0.50	0.53	0.84	0.64	0.54	0.69	0.77	0.84		
Pregabalin	0.80	0.81	0.73	0.75	0.78	0.94	-0.16	0.79	0.76	0.72	0.76		
Palbociclib	0.70	0.54	0.38	0.70	0.68	0.39	0.60	0.73	0.65	0.62	0.62		
Apixaban	0.46	-0.21	0.72	0.54	0.51	-0.26	0.74	0.40	0.38	-0.31	0.56		
Esomeprazole	0.27	0.79	0.90	0.61	0.62	0.82	0.90	0.61	0.64	0.80	0.72		
Duloxetine	0.51	0.44	-0.14	0.75	0.75	0.73	0.49	0.78	0.81	0.68	0.36		
Sofosbuvir	-0.21	0.47	0.39	0.10	0.14	0.24	0.56	-0.55	-0.54	0.35	0.40		
Guaiol	0.94	0.90	0.79	0.96	0.97	0.93	0.77	0.88	0.91	0.78	0.77		
Ferroquine	0.69	0.91	0.87	0.28	0.24	0.79	0.77	0.79	0.86	0.83	0.92		
Cu-curcumin	0.63	0.46	0.31	0.82	0.89	0.65	0.67	0.55	0.50	0.59	-0.42		
Celecoxib	0.89	0.62	0.40	0.62	0.69	0.89	0.04	0.39	0.33	0.95	-0.69		
DNIC 2	0.31	0.88	0.05	-0.02	-0.13	0.85	0.15	0.27	0.53	0.85	0.37		
Ibuprofen	0.95	0.91	0.66	0.98	0.98	0.98	0.82	0.98	0.97	0.98	0.96		
Lenalidomide	0.73	0.32	0.01	0.93	0.90	0.74	-0.28	0.71	0.68	0.82	-0.01		
Au-phosphine	0.62	0.96	0.84	0.83	0.89	0.95	0.91	0.94	0.93	0.98	0.90		
Oxycodone	0.71	0.33	-0.64	0.80	0.86	0.56	-0.69	0.59	0.65	0.71	-0.59		
Chloroquine	0.56	-0.19	0.64	0.15	0.17	-0.53	0.74	0.55	0.57	-0.46	0.63		
Aripiprazole	0.40	0.58	-0.61	0.61	0.45	0.69	0.60	0.66	0.65	0.73	0.36		
Imatinib	0.74	0.61	0.39	-0.39	-0.56	-0.30	-0.34	0.74	0.70	0.68	0.71		
Sitagliptin	0.34	0.40	0.58	0.24	0.36	0.50	0.75	0.50	0.55	0.45	0.77		
Ibrutinib	0.68	0.85	0.84	0.95	0.95	0.73	0.89	0.25	0.36	0.23	0.90		
Ru-RAPTA	0.37	0.26	0.76	0.35	0.36	0.00	0.88	-0.18	0.00	-0.68	0.97		
Ezetimibe	0.54	0.56	0.40	0.49	0.55	0.54	0.42	0.84	0.81	0.75	0.67		
Penicillin	0.20	0.79	0.78	0.52	0.48	0.88	0.73	-0.03	0.18	0.48	0.69		
Enzalutamide	0.97	0.98	0.97	0.82	0.82	0.92	0.94	0.17	0.18	0.73	0.86		
Rivaroxaban	0.88	0.82	0.83	0.95	0.93	0.98	0.90	-0.21	-0.11	0.14	-0.01		
Tenofovir	0.85	0.87	0.80	0.84	0.88	0.87	0.76	0.15	0.50	0.81	-0.11		
average	0.57	0.60	0.50	0.53	0.55	0.53	0.49	0.46	0.51	0.52	0.47		

Table S8: Computed conformational entropies S_{conf} and standard deviations **SD** in $\text{cal K}^{-1} \text{ mol}^{-1}$ at GFN2-xTB level and ALPB or GBSA in gas, *n*-hexane, and water.

molecule	gas		<i>n</i> -hexane		water			
			ALPB		GBSA	ALPB	GBSA	
	S_{conf}	SD	S_{conf}	SD	S_{conf}	S_{conf}	SD	S_{conf}
Lisdexamfetamine	21.91	1.07	19.70	2.38	21.20	22.01	0.31	22.42
Tamiflu	15.78	0.40	15.54	0.27	15.64	15.77	0.31	15.68
Ritonavir	15.34	0.17	18.37	0.37	16.97	20.04	2.52	21.46
(Z)-Rosuvastatin	15.06	0.29	7.31	0.12	7.03	9.15	0.49	8.65
Pregabalin	12.77	0.35	12.51	0.14	12.28	12.77	0.43	11.07
Palbociclib	11.17	0.20	10.50	0.23	9.15	10.50	0.50	10.50
Apixaban	10.65	0.27	10.89	0.11	11.14	11.24	0.34	10.64
Esomeprazole	10.49	0.53	10.60	0.20	11.43	11.93	0.81	11.77
Duloxetine	9.98	0.12	9.67	0.06	10.21	10.70	0.19	10.54
Sofosbuvir	9.04	0.63	10.63	0.45	11.81	11.37	0.88	11.71
Guaiol	6.49	0.34	6.21	0.06	6.96	6.52	0.09	6.81
ferroquine	5.71	0.66	2.81	1.03	4.43	4.62	0.99	6.35
Cu-curcumin	5.64	0.10	16.93	0.25	16.78	14.37	0.76	16.68
Celecoxib	4.77	0.50	4.59	0.31	4.57	2.59	0.97	4.08
DNIC 2	4.69	0.60	5.61	0.84	4.41	8.12	0.75	6.28
Ibuprofen	4.34	0.04	4.58	0.13	4.67	5.20	0.79	4.45
Lenalidomide	3.52	0.08	3.14	0.01	3.14	3.96	0.07	3.26
Au-phosphine	2.91	0.07	4.10	0.69	3.52	3.95	0.06	3.98
Oxycodone	0.30	0.00	0.31	0.01	0.21	0.57	0.08	0.82
Chloroquine	18.77	0.26	21.35	0.05	21.21	19.88	0.11	19.89
Aripiprazole	14.56	0.51	21.63	0.30	21.88	13.77	1.74	16.35
Imatinib	11.29	0.53	20.07	0.27	21.13	13.72	1.42	14.24
Sitagliptin	10.93	0.41	12.43	0.52	12.33	9.84	0.11	9.86
Ibrutinib	11.36	0.81	13.74	0.17	14.89	9.22	0.97	8.34
Ru-RAPTA	6.96	0.13	9.45	0.74	8.51	8.97	0.3	10.57
Ezetimibe	9.18	0.47	10.02	0.19	9.52	12.20	0.23	12.96
Penicillin	7.73	0.31	8.34	0.24	9.25	12.04	0.45	12.06
Enzalutamide	6.08	0.29	7.75	0.20	7.18	8.43	0.73	8.23
Rivaroxaban	5.78	0.19	5.99	0.30	8.06	7.25	0.80	9.05
Tenofovir	4.56	0.08	4.85	0.17	4.49	6.45	1.06	2.83
average	9.26	0.35	10.32	0.36	10.47	10.24	0.64	10.38

Table S9: Computed conformational entropies S_{conf} and standard deviations **SD** in $\text{cal K}^{-1} \text{ mol}^{-1}$ at GFN1-xTB and GFN-FF levels (+ ALPB) in gas, *n*-hexane, and water.

molecule	GFN1						GFN-FF					
	gas		<i>n</i> -hexane		water		gas		<i>n</i> -hexane		water	
	S_{conf}	SD										
Lisdexamfetamine	20.92	0.26	21.01	0.08	20.50	2.23	10.54	0.20	14.01	0.32	17.03	1.07
Tamiflu	16.74	0.07	18.28	0.39	17.83	0.41	14.63	0.37	16.08	0.43	16.79	0.41
Ritonavir	17.5	0.66	17.43	0.2	13.36	1.26	16.92	0.49	15.85	0.87	16.64	0.41
(z)-Rosuvastatin	9.39	0.10	10.11	0.18	15.67	0.51	8.97	0.81	10.87	0.75	14.82	0.61
Pregabalin	16.29	1.62	12.45	1.91	5.61	0.30	9.10	0.47	11.03	0.46	12.30	0.14
Palbociclib	9.99	0.40	8.60	0.26	10.30	0.51	8.71	0.21	9.00	0.60	8.53	0.26
Apixaban	10.56	0.11	10.35	0.21	10.76	0.37	9.82	0.07	10.81	0.20	11.83	2.06
Esomeprazole	15.41	0.11	12.27	0.40	14.87	0.23	12.10	0.50	14.46	0.74	14.17	0.70
Duloxetine	12.70	0.12	10.42	0.30	11.51	0.40	10.77	0.18	9.90	1.09	12.80	0.20
Sofosbuvir	11.97	0.16	11.96	0.31	14.29	0.23	4.67	0.40	8.45	2.34	5.85	0.95
Guaiol	5.82	0.06	5.43	0.06	5.15	0.03	3.80	0.10	4.31	0.67	4.04	0.05
Ferroquine	9.52	0.28	10.96	0.42	10.83	0.61	3.11	0.25	9.09	0.66	5.27	1.47
Cu-curcumin	10.06	0.99	16.50	0.35	17.93	1.25	15.89	0.43	17.02	0.23	21.47	0.75
Celecoxib	4.55	0.13	6.05	0.78	4.77	0.39	3.97	0.49	4.96	0.87	6.88	1.03
DNIC 2	8.68	1.02	11.55	0.13	6.98	0.84	8.14	1.38	10.21	0.62	12.94	2.83
Ibuprofen	4.90	0.03	4.83	0.16	5.61	0.69	5.74	0.22	5.82	0.17	6.32	0.30
Lenalidomide	4.22	0.30	4.94	0.24	2.89	0.30	5.19	0.56	3.37	0.69	3.49	0.73
Au-phosphine	3.02	0.30	3.43	0.61	2.31	0.85	6.65	0.60	7.06	0.28	6.90	0.37
Oxycodone	0.58	0.08	0.73	0.09	2.22	0.48	2.38	0.21	1.93	0.23	2.32	0.10
Chloroquine	16.41	0.17	18.47	0.13	18.54	0.43	11.94	0.19	13.68	0.38	11.54	0.16
Aripiprazole	13.80	0.08	18.40	0.09	16.97	1.39	14.58	0.15	14.77	0.29	15.61	0.30
Imatinib	12.37	0.11	16.90	0.57	11.61	0.65	13.03	0.23	15.45	0.26	14.76	0.29
Sitagliptin	12.71	0.36	14.88	0.56	6.05	0.56	9.78	0.49	15.62	0.93	16.16	0.72
Ibrutinib	9.77	0.56	12.77	1.02	11.71	0.33	8.94	0.37	12.01	0.88	13.66	0.26
Ru-RAPTA	10.66	0.68	12.39	0.36	6.29	0.24	14.86	0.09	15.29	0.13	13.44	0.20
Ezetimibe	8.04	0.38	13.68	0.45	9.95	1.77	10.06	0.65	7.60	1.24	12.16	1.00
Penicillin	5.55	0.25	8.26	0.17	9.05	0.17	8.03	0.66	9.74	1.17	7.13	1.62
Enzalutamide	5.64	0.18	6.37	0.29	8.18	0.34	4.36	0.19	6.27	0.64	8.44	1.93
Rivaroxaban	5.40	0.26	7.03	0.31	10.91	0.17	8.53	0.60	8.50	0.36	8.95	0.56
Tenofovir	1.64	0.14	6.96	0.45	7.51	2.34	4.73	0.03	4.56	0.07	12.52	0.59
average	9.83	0.33	11.11	0.38	10.34	0.68	9.00	0.38	10.26	0.62	11.16	0.74

Table S10: Empirical molecular flexibility measure ξ_f at GFN2-xTB, GFN1-xTB and GFN-FF levels and number of atoms N_{atoms} for all molecules of the CD30 set.

	N_{atoms}	GFN2			GFN1			GFF		
		gas	<i>n</i> -hexane	water	gas	<i>n</i> -hexane	water	gas	<i>n</i> -hexane	water
Lisdexamfetamine	44	0.45	0.55	0.47	0.48	0.50	0.54	0.45	0.46	0.46
Tamiflu	50	0.49	0.50	0.49	0.50	0.50	0.50	0.47	0.48	0.48
Ritonavir	98	0.39	0.40	0.39	0.39	0.40	0.40	0.35	0.35	0.35
(Z)-Rosuvastatin	61	0.31	0.34	0.34	0.34	0.34	0.37	0.32	0.32	0.33
Pregabalin	28	0.58	0.58	0.58	0.58	0.58	0.70	0.52	0.52	0.52
Palbociclib	62	0.19	0.19	0.18	0.20	0.20	0.20	0.24	0.24	0.23
Apixaban	59	0.18	0.18	0.18	0.18	0.18	0.18	0.19	0.19	0.19
Esomeprazole	43	0.37	0.38	0.37	0.35	0.36	0.35	0.38	0.36	0.32
Duloxetine	40	0.41	0.41	0.41	0.41	0.42	0.42	0.38	0.40	0.38
Sofosbuvir	65	0.40	0.40	0.39	0.35	0.35	0.34	0.32	0.33	0.33
Guaiol	42	0.23	0.23	0.23	0.23	0.23	0.23	0.23	0.23	0.23
Ferroquine	52	0.30	0.30	0.29	0.32	0.32	0.33	0.26	0.27	0.26
Cu-curcumin	53	0.20	0.19	0.19	0.19	0.20	0.20	0.21	0.34	0.22
Celecoxib	40	0.15	0.15	0.15	0.15	0.15	0.15	0.16	0.16	0.16
DNIC 2	24	0.65	0.65	0.65	0.47	0.47	0.66	0.50	0.52	0.52
Ibuprofen	33	0.34	0.34	0.34	0.34	0.34	0.34	0.34	0.34	0.34
Lenalidomide	32	0.13	0.13	0.13	0.13	0.13	0.13	0.14	0.14	0.14
Au-phosphine	39	0.23	0.23	0.23	0.23	0.24	0.23	0.20	0.23	0.23
Oxycodone	44	0.16	0.16	0.17	0.17	0.17	0.17	0.16	0.16	0.16
Chloroquine	48	0.44	0.45	0.45	0.49	0.49	0.49	0.40	0.40	0.39
Aripiprazole	57	0.39	0.40	0.40	0.40	0.40	0.40	0.32	0.32	0.35
Imatinib	68	0.23	0.23	0.22	0.24	0.25	0.24	0.21	0.22	0.21
Sitagliptin	43	0.31	0.32	0.32	0.32	0.32	0.32	0.27	0.27	0.33
Ibrutinib	57	0.18	0.17	0.18	0.18	0.18	0.18	0.19	0.19	0.19
Ru-RAPTA	59	0.25	0.25	0.29	0.28	0.28	0.27	0.26	0.24	0.24
Ezetimibe	51	0.32	0.32	0.32	0.28	0.29	0.32	0.26	0.28	0.28
Penicilin	41	0.29	0.29	0.29	0.29	0.29	0.29	0.30	0.30	0.30
Enzalutamide	48	0.12	0.12	0.11	0.12	0.12	0.12	0.16	0.16	0.16
Rivaroxaban	47	0.28	0.29	0.28	0.29	0.29	0.29	0.28	0.30	0.27
Tenofovir	33	0.33	0.34	0.45	0.17	0.35	0.35	0.30	0.30	0.30

References

- (S1) Still, W. C.; Tempczyk, A.; Hawley, R. C.; Hendrickson, T. *J. Am. Chem. Soc.* **1990**, *112*, 6127–6129.
- (S2) Onufriev, A. V.; Case, D. A. *Annu. Rev. Biophys.* **2019**, *48*, 275–296.
- (S3) Pracht, P.; Grimme, S. *Chem. Sci.* **2021**, *12*, 6551–6568.
- (S4) Bursch, M.; Kunze, L.; Vibhute, A. M.; Hansen, A.; Sureshan, K. M.; Jones, P. G.; Grimme, S.; Werz, D. B. *Chem. Eur. J.* **2021**, *27*, 4627–4639.

- (S5) Grimme, S.; Hansen, A.; Ehlert, S.; Mewes, J.-M. *J. Chem. Phys.* **2021**, *154*, 64103.
- (S6) Klamt, A. *J. Phys. Chem.* **1995**, *99*, 2224–2235.
- (S7) Klamt, A.; Jonas, V.; Bürger, T.; Lohrenz, J. C. W. *J. Phys. Chem. A* **1998**, *102*, 5074–5085.
- (S8) Grimme, S.; Bohle, F.; Hansen, A.; Pracht, P.; Spicher, S.; Stahn, M. *J. Phys. Chem. A* **2021**, *125*, 4039–4054.
- (S9) Eckert, F.; A. Klamt, COSMOtherm, version C3.0, release 16.01; COSMOlogic GmbH & Co. KG: Leverkusen, Germany, 2016.
- (S10) Balasubramani, S. G.; Chen, G. P.; Coriani, S.; Diedenhofen, M.; Frank, M. S.; Franzke, Y. J.; Furche, F.; Grotjahn, R.; Harding, M. E.; Hättig, C.; Others, *J. Chem. Phys.* **2020**, *152*, 184107.
- (S11) Ahlrichs, R.; Bär, M.; Häser, M.; Horn, H.; Kölmel, C. *Chem. Phys. Lett.* **1989**, *162*, 165–169.
- (S12) Treutler, O.; Ahlrichs, R. *J. Chem. Phys.* **1995**, *102*, 346–354.
- (S13) Eichkorn, K.; Treutler, O.; Öhm, H.; Häser, M.; Ahlrichs, R. *Chem. Phys. Lett.* **1995**, *242*, 652–660.
- (S14) Weigend, F. *Phys. Chem. Chem. Phys.* **2006**, *8*, 1057.
- (S15) Kuhn, B.; Mohr, P.; Stahl, M. *J. Med. Chem.* **2010**, *53*, 2601–2611.
- (S16) Humphrey, W.; Dalke, A.; Schulten, K. *J. Mol. Graph.* **1996**, *14*, 33–38.
- (S17) Spicher, S.; Grimme, S. *Angew. Chem. Int. Ed.* **2020**, *59*, 15665–15673.
- (S18) Spicher, S.; Plett, C.; Pracht, P.; Hansen, A.; Grimme, S. *J. Chem. Theory Comput.* **2022**, accepted.